

Flexural Modulus Enhancement and Minimization of Printing Time and Part Weight for PET-G, Using Taguchi-GRA-TOPSIS Techniques

MOHAMMED RAFFIC N.^{1*}, GANESH BABU K.², RAJASEKARAN SAMINATHAN³, HAITHAM HADIDI³

¹Department of Food Technology, Nehru Institute of Technology, Coimbatore, India

²Department of Mechanical Engineering, Chendhuran College of Engineering and Technology, Pudukkottai, India

³Department of Mechanical Engineering, Jazan University, Kingdom of Saudi Arabia

Abstract: Fused deposition modeling (FDM) is becoming the most promised additive manufacturing (AM) process in recent years due to the evident benefits, such as high design flexibility, low cost, friendly and economically use. The current study considers an optimization of four different FDM parameters varied in three levels, as layer thickness (0.17 mm, 0.25 mm and 0.33 mm), infill density (25, 50 and 75%), shell thickness (0.8 mm, 1.2 mm and 1.6 mm) and raster angle (0°, 30° and 60°) with an objective to reduce printing time, part weight and to enhance flexural modulus using Polyethylene Terephthalate - glycol modified (PET-G) material. Mono optimization of FDM input parameters has been done using signal to noise ratio method obtained from Taguchi's L₉ Orthogonal Array (OA) and multi response optimization is applied through Grey Relational Analysis (GRA) and technique of order preference similar to ideal solution (TOPSIS) techniques. The response or its criteria weightages are calculated using Shanon's entropy and CRITIC method which gives different weightages for the considered responses. Printing time ranks top with 37% from entropy method followed by flexural modulus with 36% and part weight ranks last with 28%. Flexural modulus ranks tops with 43% followed by part weight with 29% and printing time takes last position with 28% weightage through CRITIC method. The ranking of alternatives from GRA- entropy and GRA- CRITIC methods are similar by recommending A1B1C1D1 (0.17 mm layer thickness, 25% infill density, 0.8 mm shell thickness and 0° raster angle) but TOPSIS-entropy and TOPSIS – CRITIC methods suggested different parameter combination A2B3C1D2 (0.25 mm layer thickness, 75% infill density, 0.8 mm shell thickness and 30° raster angle). From all the four different methods adopted for optimization, the parameter setting obtained from level total suggests A2B1C1D2 (0.25 mm layer thickness, 25% infill density, 0.8mm shell thickness and 30° raster angle) and completely opposite to the ranking of alternatives. The carried - out confirmation trials carried out validated the optimized settings resulted from different methods. Infill density is found to be the most significant factor as compared to other input factors over the output assessed parameters

Keywords: Fused Deposition Modeling, Taguchi's Orthogonal Array, PET-G, flexural modulus, GRA, TOPSIS (technique of order preference similar to ideal solution)

1. Introduction

Manufacturing industries always strive hard to boost productivity at low cost with more effectiveness and efficiency, every time when they proceed to bring out products to the market. Customized product manufacturing always induces higher manufacturing cost and material wastage as the size of the production volume is small in number. The current industrial revolution 4.0 includes the manufacturing of product through digital means and the umbrella term for all the digital product manufacturing is termed as additive manufacturing (AM). Additive manufacturing has addressed the challenges faced by the manufacturing industry for many decades through traditional manufacturing routes, such as subtractive and formative manufacturing. AM techniques functions with a common framework, where

*email: drmrffnoor@gmail.com



the product gets manufactured from a CAD file irrespective of the raw material form and principle involved in conversion process. AM techniques create the parts in a layer-by-layer fashion, as per the predetermined path specified by the slicing software. AM techniques have gained more prominence as they can be achieved through methods, such as extruding a molten material, powder solidification, joining particles of material, solidifying liquid polymer and layer bonding [1]. The synonymous terms for AM include additive fabrication, layer manufacturing, freeform fabrication and additive layer manufacturing [2]. Fused deposition modeling is an extensive additive manufacturing technique for the creation of parts with high degree of complexity with diverse materials such as thermoplastics, fibre reinforced composites, metals and ceramics. FDM process is based on the principle of thermal energy, surface chemistry and layer manufacturing advanced technique [3]. Started its journey during 1980's as a toy manufacturing process, it has seen tremendous growth today to serve industries such as aerospace, architecture, automotive, bio-medical and smart home [4]. The process offers numerous positive benefits to the end user such as being user friendly in operation, low difficulty in handling, less cost and material waste, high design freedom, customized design, increase in material options day by day led this technique to be considered for domestic and industrial production [5,6]. The FDM process involves multitude parameters which has influence over the final printed part and it need to be optimized through standard methodology to ensure the printed part meets the demand of the customer. Despite the positive benefits of FDM stated earlier, parts created though FDM still exhibits inferior performance under different aspects such as mechanical properties, surface finish, dimensional accuracy, production time than conventional manufacturing techniques of thermoplastics such as injection moulding [7]. Researchers all around the globe are showing more interest in conducting detailed research to ascertain the significant influence of FDM process parameters to obtain equal or superior part characteristics than the parts processed through conventional means. Srinivasan et.al [8] varied infill density to understand its effect over the tensile strength and surface roughness of the part made out of PET-G by maintaining other parameters at constant level. The authors have printed the tensile test specimen as per ASTM D638 standard using WOL 3D ender and reported that increase in infill density increases the tensile strength of the specimen at 0.1 mm layer thickness with grid pattern and surface roughness decreases considerably. Juan et.al [9] involved in studying the properties of PET-G for enhancing the surface finish and hydrophobicity by varying the factors such as layer height, print temperature, print speed, print acceleration and flow rate in three levels to form the L_{27} orthogonal array. The research is targeted towards manufacture of LED spotlights through FDM using PET-G material as potential candidate. The experimental results have been analyzed through ANOVA and it has revealed that flow rate, print acceleration has the greatest influence than other factors considered for study. Santos et.al [10] adopted FDM process to print PET-G and PLA material for analyzing their potential to acts as sacrificial claddings for protection from impact forces. The materials are examined in the form of honeycomb and auxetic structures placed in between terminal stiffening plates to observe the one exhibiting higher energy dissipation ratio and lower restitution coefficient PET-G exhibited superior performance than PLA and also found to be suited for manufacturing protection gears through low cost FDM printers. Srinivasan et al. [11] varied the FDM parameters such as infill density, infill pattern and layer thickness to measure the tensile strength and surface roughness values. The authors have considered PET-G material for the experimentation and reported that increase in infill density increases the tensile strength and reduces surface roughness. Grid pattern has resulted with very smooth surface compared to other patterns involved. Ajay Kumar et al. [12] experimented carbon fibre reinforced PET-G thermoplastics by varying the parameters such as print speed, layer thickness and infill density to understand their influence over the tensile, flexural and hardness properties. The experimental values have been analyzed through multi response optimization and regression equations have been created. Both print speed and layer height are significant in terms of tensile strength, print speed and infill density are significant in terms of hardness and no factor selected or examined is significant over flexural strength measured. Srinivasan et al. [13] analyzed the effect of nine different infill patterns such as triangular, grid, cubic, honeycomb, concentric, rectilinear, rectangular, octet and wiggle over the tensile strength of PET-G

specimens. Grid pattern and honeycomb pattern have exhibited tensile strength of 36.34 MPa, 34.26 MPa, respectively, and concentric infill pattern resulted with lowest tensile strength of 13.54 MPa due to interlayer non availability. Muammel et al. [14] evaluated anisotropy of PET-G specimens by varying the raster angles, printing orientation and infill percentage through tensile testing. From the studies carried out, higher tensile strength is obtained for 0° raster orientation and part orientation in Y direction for PET-G material compared to PLA. Arda et al. [15] conducted mechanical characterization of FDM printed PET-G specimens through tensile testing and reported that the slicing technique adopted has a great influence over the final product's performance. The mode of fracture observed for PET-G is brittle at room temperature. Durgashyam et al. [16] exploited the benefits of testing standards ASTM D638 and ASTM D670 for measuring the tensile, flexural properties of PET-G material by varying the parameters such as layer thickness, infill density and flow rate. The experimental results have been statistically analyzed through ANOVA and authors have reported that contribution of layer thickness is higher for both tensile strength and flexural strength with 57.82 and 41.87% than other parameters considered. Srinidhi et al. [17] reported about the performance of PET-G and Carbon fibre reinforced PET-G material by measuring their tensile, impact, hardness and flexural properties as per standard sized specimens. The research carried out involves post processing of specimens through annealing at a temperature of 100°C held for 60 min to ascertain the improvement in properties for different infill patterns. The research findings have shown an acceptable improvement in properties of both the materials considered and CFR-PETG has shown superior performance than its counterpart PET-G for the conditions tested out. Ming et al. [18] explored the effect of FDM parameters such as printing speed and printing temperature over the thermal and mechanical properties of materials such as PLA and PET-G. The authors have conducted tensile, compressive and bending test for the specimens printed to evaluate their mechanical properties and thermal deformation test for measuring the thermal properties of the specimen. The outcomes are quite opposite for the mechanical and thermal properties of the both the materials. PLA has superior mechanical properties than PET-G and PET-G revealed better thermal properties than PLA. Jorge et al. [19] implemented both experimental investigation and numerical analysis of PET-G polymers for evaluating their suitability for architectural applications and reported PET-G as a viable material for industrial applications through proper selection of input parameters. Zen et.al [20] experimentally evaluated the role of FDM manufacturing parameters such as layer thickness, overlap ratio over the microstructure formed and mechanical properties of PET-G material. The authors have reported that a low value of layer thickness and higher overlap ratio has reduced internal porosity and shown improvement in mechanical properties of the material studied. Dinesh et.al [21] applied the concept of Adaptive Neuro Fuzzy Inference System (ANFIS) for analyzing the significant FDM parameters for ABS, PET-G and multimaterial by evaluating the tensile strength of specimens printed considering extrusion temperature, material density and layer height. PETG has shown the maximum tensile strength than ABS material at 225°C extrusion temperature and 0.1 mm layer height. The experimental data obtained are trained using ANFIS and the results obtained are found to have a low error percentage (2.63%). Mohammed Raffic et al. [22] applied the concepts of Taguchi orthogonal array, Grey relational analysis and TOPSIS to study the effect of FDM parameters such as slice height, infill density, shell thickness and raster angle for HIPS material and reported that the influencing parameter over flexural strength varies according to the method considered for evaluation. Ganesh Babu et al. [23] exploited the benefits of experimental design and range analysis to optimize FDM parameters for materials such as PET-G, PLA and HIPS for enhancing fatigue strength and minimizing part weight. The authors have reported infill density as highly influencing. Mohammed Raffic et al. [24] conducted parametric optimization study for ABS material for predicting the fatigue life of FDM printed ABS material through designed experiments. Ganesh babu et al. [25] performed multi response optimization of FDM parameters using grey relational analysis and Data envelopment analysis based ranking methods for ABS samples to study the effect of FDM parameters over model building time, part weight and compression strength. Haitham Hadidi et.al [26] shot peened the printed layers of P430 ABS material to improve the energy absorbing characteristics and resist fracture. The study carried out has revealed that

both layer peening frequency and printing orientation has strong influence over controlling the desired part characteristics. The literature review gives a fair concluding remark that fused deposition modeling is a research area of growing interest which has paved the way for the development of many feasible materials which finds applications in diverse industrial sectors. The literal way of conducting research in FDM is the evaluation of various static and dynamic mechanical properties, determination of dimensional accuracy, printing time, and material consumption, assessing the surface quality of end parts for further post processing, optimization of process parameters to make the material suitable to address or overcome the existing problems in conventional manufacturing. The current study considers flexural modulus as an index for the evaluation of mechanical property and also printing time, part weight resulted in the printing process by using PET-G filament through Taguchi's orthogonal array. The results are subjected for optimizing input parameters through mono and multi response optimization techniques to obtain the significant parameter and optimized combination of input factors.

2. Materials and methods

The humongous development of materials catering the needs of diverse applications has made mankind to live a safe and more sophisticated life than the past. The study involves PET-G filaments for the printing of specimens through FDM process to explore the properties for further consideration on viable industrial applications.

2.1. Polycarbonate filament

PET- G is glycol modified version of Polyethylene Terephthalate, G stands for Glycol which is added at molecular level to offer chemical properties. As a copolymer it combines PET and Glycol which overcomes the overheating issues resulted with PET. PET-G is produced by a simple two step melt phase poly condensation process using the monomers together with a release of water molecule. As comparing to PET, PET-G has higher durability, greater strength and impact resistance, capability to withstand high temperatures. The competitive advantages of PET-G in comparison to its counterparts in 3D printing, such as ABS and PLA, has seen an increased uptake in the global market. PET can be easily printed with excellent layer adhesion and low shrinkage rate than PLA and ABS. PETG can be injection moulded, extruded in sheet or filament form for making products. Being strong, cost effective, recyclable, food safe, colorable, non toxic and providing odorless emissions makes PET-G highly suitable for 3D printing. PETG finds applications in making of machine guards, medical and pharmaceutical applications, retail stands and displays, food and drink containers. PET-G filaments are available in colors such as black, blue, green, grey orange and white in two different diameters such as 1.75 mm and 2.85 mm for FDM. Table 1 shows the different physical and mechanical properties of PET-G filament.

Table 1. Various properties of PET-G FDM filament

No	Property / Characteristic	S.I Unit	Value
1	Density	g/cm ³	1.23
2	Toughness	Kj/m ²	7.3
3	Tensile modulus	GPa	2.1
4	Tensile strength	MPa	45.8
5	Elongation at break	%	18
6	Hardness	D Scale	85
7	Glass transition temperature	°C	82

2.2. Taguchi's orthogonal array

Experimental design in research always considered for reducing the MTR (money, time and resources) involved without compromising the quality desired in output or characteristic measured out. Taguchi's orthogonal array (OA) design is a type of general fractional factorial design that is based on a design matrix proposed by Genichi Taguchi and allows you to consider a selected subset of combinations of multiple factors at multiple levels. Taguchi orthogonal arrays are balanced to ensure that all levels of all factors are considered equally. The current work considers four different FDM input parameters such as layer thickness, infill density, raster angle and shell thickness varied in three levels for conducting 9 different treatments as per L_9 orthogonal array. Layer thickness represents the thickness of individual layers deposited one over the another and for 0.4mm dia extrusion nozzle layer thickness may be varied from 0.1mm to 0.33mm. Infill density denotes the amount of material added which can be varied from 0% to 100% based upon the type of model printed. Shell thickness has a linear relationship with nozzle diameter and it adds material to the model when strength is of prime importance. Raster angle indicates the angle of individual raster deposited with respect to horizontal axis. The parameters considered and their levels varied are indicated in Table 2. Table 3 shows the output parameters measured and the experimental design layout for conducting different treatments are shown in Table 4.

Table 2. FDM Input parameters and their levels varied

S. No	Input Factors	Symbol	Unit	Level 1	Level 2	Level 3	Level 1	Level 2	Level 3
1	Layer thickness	A	mm	-1	0	1	0.17	0.25	0.33
2	Infill density	B	%	-1	0	1	25	50	75
3	Shell thickness	C	mm	-1	0	1	0.8	1.2	1.6
4	Raster angle	D	°	-1	0	1	0	30	60

Table 3. Output parameters and their objectives

S. No	Output Factors	Symbol	Unit	Category	Objective
1	Printing time	PT	mins	Non beneficial	Minimize
2	Part weight	PW	gms	Non beneficial	Minimize
3	Flexural Modulus	FM	GPa	Beneficial	Maximize

Table 4. Experimental design matrix as per L_9 OA

S. No	A (mm)	B (%)	C (mm)	D (°)
1	0.17	25	0.8	0
2	0.17	50	1.2	30
3	0.17	75	1.6	60
4	0.25	25	1.2	60
5	0.25	50	1.6	0
6	0.25	75	0.8	30
7	0.33	25	1.6	30
8	0.33	50	0.8	60
9	0.33	75	1.2	0

2.3. RAISE 3D- FDM printer

The printing of PET-G specimens for experimentation is done by using professional RAISE3D PRO 2 series (ISO 9001 and 14001 certified) which is compatible in printing FDM materials such as PLA/ ABS/ HIPS/ PC/ TPU/ TPE/ PETG/ ASA/ PP/ PVA/ Nylon/ Glass Fiber Infused/ Carbon Fiber Infused/ Metal Fill/ Wood Fill. The machine has a build volume of 305 mm × 305 mm × 300 mm (l x b x h) with

maximum build plate temperature of 110°C and maximum nozzle temperature of 300°C. The machine functions better with idea maker slicing software for creating printed models from.stl files. The machine prints the model inside an enclosed chamber by extruding the filament through a heated nozzle and deposits over the heated bed in layer by layer fashion. Figure 1 shows the raise3D FDM machine used for printing the specimens.

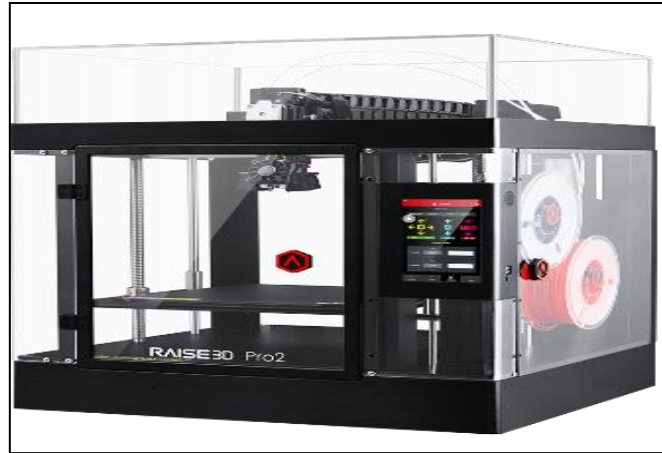


Figure 1. RAISE 3D Pro 2 Series FDM Printer

2.4. Experimental procedure

The evaluation of flexural strength of the printed specimen is done by conducting three point bending test which involves loading the printed specimen at the mid span by supporting at both the ends. The test is continued until the specimen undergoes fracture or attains a permanent bend in its structure. The maximum load withstood by the specimen and displacement undergone are taken for the calculation of flexural strength. The displacement occurred due to the applied load is recorded through the data acquisition system provided in the test setup and utilized for finding flexural strain. A flat specimen of size 250 mm (L) x 20 mm (B) x 10 mm (H) is printed. Figure 2 shows the 2D and 3D views of flexural specimen used in the current study.

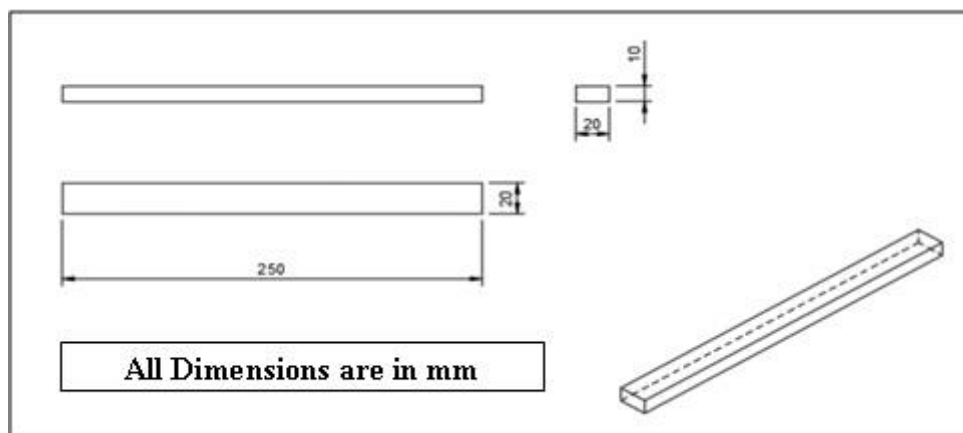


Figure 2. PET-G Flexural Test Specimen

The specimen modeling is carried using CATIA V5 software and stored in.stl format for slicing the same using ideamaker software version 4.2.2. The slicing software has capabilities for varying the parameters such as layer thickness, infill density, raster angle, shell thickness or no of shells, printing speed, different process temperatures such as extrusion temperature, envelope temperature and bed temperature. The sliced specimen with varied input factors have been fed to the machine for proceeding the specimen preparation in layer by layer fashion. The schematic representation of three point bending

test setup is shown in Figure 3. The supports have been placed with a distance of 25mm from both the ends underneath the specimen.

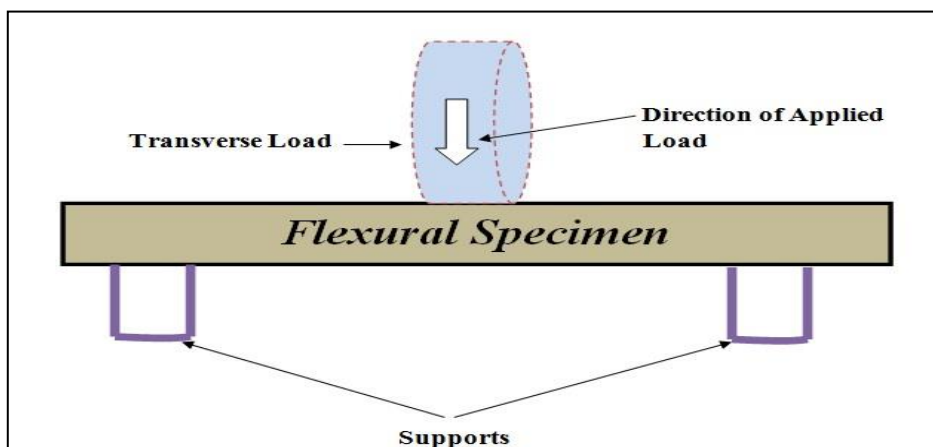


Figure 3. Schematic representation of three - point bending test (or) flexural test

Table 5. Three Point Bending Test Experimental Observations

S.No	A (mm)	B (%)	C (mm)	D (°)	Flexural Force (N)	Displacement (mm)
1	0.17	25	0.8	0	1326	30.16
2	0.17	50	1.2	30	1863	28.17
3	0.17	75	1.6	60	2262	31.02
4	0.25	25	1.2	60	1707	39.20
5	0.25	50	1.6	0	1521	32.92
6	0.25	75	0.8	30	2775	33.43
7	0.33	25	1.6	30	1581	35.62
8	0.33	50	0.8	60	1644	32.80
9	0.33	75	1.2	0	516	15.31



Figure 4. Fractured FDM printed PET-G Specimens - three - point bending test

The values observed for the flexural testing of PET-G specimens are tabulated in Table 5 as flexural force withstood by the specimen and the corresponding displacement occurred. The fractured PET-G specimens are shown in Figure 4.

3. Results and discussions

The value of flexural modulus is obtained from the ratio of flexural strength and flexural strain and the values of flexure strength and flexural strain is obtained from equations 1 and 2. The signal to noise ratio values are calculated as per the objective of the output response such as higher the better (Flexural modulus) and lower the better (Printing time, Part weight) as mentioned in equations 3 and 4.

$$\sigma_f = \frac{3PL}{2wd^2} \quad (1)$$

$$\varepsilon_f = \frac{6Dd}{L^2} \quad (2)$$

σ_f - Flexural stress, GPa

ε_f - Flexural strain

P – Load, N

L - Length of the beam, mm

w - width of the beam, mm

d - Thickness of the beam, mm

For higher the better case - $S/N = - 10 \cdot \log (\Sigma (1/Y^2)/n)$ (3)

For lower the better case - $S/N = - 10 \cdot \log (\Sigma(Y^2)/n)$ (4)

n - no of experimental trials

The calculated signal to noise ratio values as per equation 3 and 4 for the output parameters are shown in Table 6.

Table 6. Output parameters printing time, part weight, flexural modulus and their signal to noise ratio values

Trial No	A (mm)	B (%)	C (mm)	D (°)	PT (mins)	PW (gms)	FM (GPa)	SNR PT	SNR PW	SNR FM
1	0.17	25	0.8	0	117	23.1	8.59	-41.36	-27.27	18.68
2	0.17	50	1.2	30	168	34.8	12.92	-44.51	-30.83	22.22
3	0.17	75	1.6	60	213	45.5	14.24	-46.57	-33.16	23.07
4	0.25	25	1.2	60	98	26.7	8.51	-39.82	-28.53	18.59
5	0.25	50	1.6	0	128	37.3	9.02	-42.14	-31.43	19.11
6	0.25	75	0.8	30	143	45.5	16.21	-43.11	-33.16	24.2
7	0.33	25	1.6	30	85	29.6	8.67	-38.59	-29.43	18.76
8	0.33	50	0.8	60	94	36.3	9.79	-39.46	-31.2	19.82
9	0.33	75	1.2	0	116	45.9	6.58	-41.29	-33.24	16.37

The values of flexural modulus of the printed PET-G specimen has been calculated from the values of flexural strength and flexural strain attained using the equations 1 and 2. The calculated values for the respective trials has been tabulated to understand the variation shown by the specimen due to the

changes in combination of input parameters studied. The lowest values of printing time and part weight has been attained in different experimental trials. Experiment number 7 with 0.33 mm layer thickness, 25% infill density, 1.6 mm shell thickness and 30° raster angle has 85 min for printing the specimen with 29.6 g of part weight and 8.67 GPa flexural modulus. Comparing to the maximum printing time given by experiment 3 (0.17 mm layer thickness, 75% infill density, 1.6 mm shell thickness and 60° raster angle), it shows a reduction of printing time by 63%. With respect to the lowest part weight of 23.1 g, the part weight obtained at lowest printing time of 85 min is found to be 22% higher. In comparison to the maximum flexural modulus of 16.21 GPa, the setting which gives lowest printing time of 85 min has shown a reduction of 46.51%. Focussing upon the objective of lowest part weight the experiment number 1 (0.17 mm layer thickness, 25% infill density, 0.8 mm shell thickness and 0° raster angle) has resulted with 23.1 g of part weight attained in a printing time of 117 min with a flexural modulus value of 8.59 GPa. Comparing to the highest part weight resulted from experiment number 9 (0.33 mm layer thickness, 75% infill density, 1.2 mm shell thickness and 0° raster angle), experiment number 1 shows part weight reduced by 49.67 % with an increase of printing time by 37.64% with respect to lowest printing time 85 min and 82.05% decrease while comparing with the maximum printing time of 213 min. To attain maximum flexural strength of the specimen printed to deploy the printed part in applications demanding high flexural strength experiment number 6 (0.25 mm layer thickness, 75% infill density, 0.8 mm shell thickness and 30° raster angle) has shown 16.21 GPa for the specimen experimented. In comparing to the lowest flexural modulus value of 6.58 GPa from experiment number 9 (0.33 mm layer thickness, 75% infill density, 1.2 mm shell thickness and 0° raster angle) flexural modulus has got increased by 146.35 % with an increase of printing time by 68.25% with respect to lowest printing time of 85 min and decrease by 48.91% with the maximum printing time of 213 min, with no changes in specimen weight. In case of part weight for the specimen exhibited maximum flexural modulus it shows an increase of 96.96% with respect to lowest part weight of 23.1 g and just 0.87% increase with the maximum part weight of 45.9 g. The detailed comparative analysis carried out gives a crystal clear idea about the combination of parameter settings to be adopted for attaining the output responses along with their objective by compromising the objectives of other output responses studied.

3.1. Mono optimization

Optimization plays a vital role in identifying set of parameters which can enhance or reduce a property based upon the desire and also identifies the significant parameter influencing the output characteristics studied.

3.2. Printing time

The values of the output parameters measured have been converted as signal to noise ratio values as per the objective stated earlier. The time for printing falls under the category of minimization and the corresponding response table values are shown in Table 7.

Table 7. Response table values for printing time

Level	A (mm)	B (%)	C (mm)	D (°)
1	-44.15	-39.93	-41.31	-41.60
2	-41.69	-42.04	-41.87	-42.07
3	-39.78	-43.65	-42.43	-41.95
Delta	4.37	3.73	1.12	0.47
Rank	1	2	3	4

For reducing the printing time involved in making the specimen, it is understood from main effect plot generated through Minitab 17.0 software, that the input parameter combination 0.33 mm layer thickness, 25% infill density, 0.8 mm shell thickness and raster angle of 0° needs to be selected. The

recommended setting may be adopted for the applications which require the printing time reduction for reducing the lead time involved. The setting may reduce the time by affecting the specimen weight and other properties of the product which has to be considered before adoption for avoiding potential consequences. As for the response table values, layer thickness seems to be the most significant factor affecting printing time, followed by infill density, shell thickness and raster angle. The surface roughness of the part increases when higher layer thickness values are considered which is the major downside of this setting. Figure 5 shows the main effect plot for obtaining reduced printing time of the part.

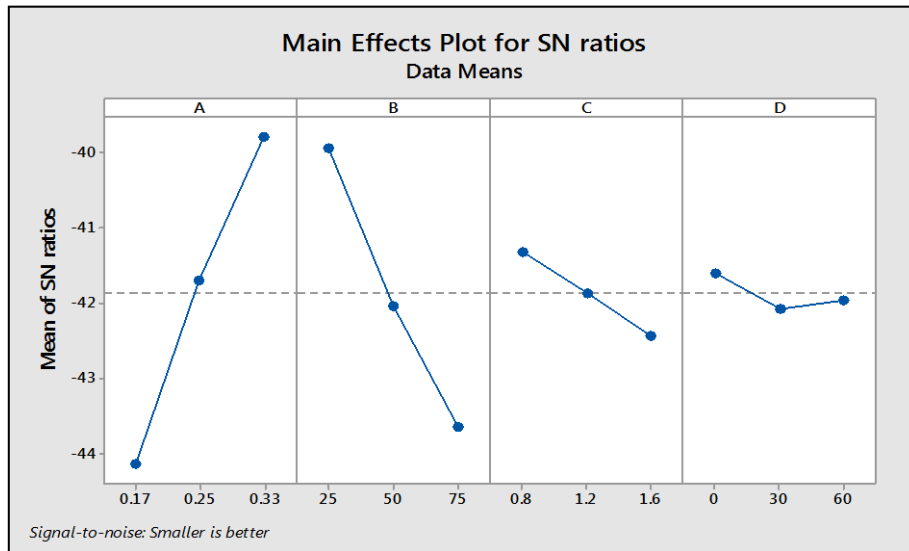


Figure 5. Main effect plot for reduced printing time

3.3. Part weight

Weight reduction of a component is always the most demanded criteria in many applications such as aeronautical, automotive and civil engineering. The main effect plot has shown the combination 0.17 mm layer thickness, 25% infill density, 0.8 mm shell thickness and raster angle of 0° for obtaining the lowest specimen weight and the obtained setting is already available with the experimental trial. Low weighed parts are in high demand for the creation of visual prototypes. The response table values indicate the same combination of input parameter setting. Infill density ranks top in controlling the part weight, followed by layer thickness, shell thickness and raster angle. The strength of the part goes down through this setting which is the major downside and Table 8 shows the response table values for part weight. Figure 6 shows the main effect plot for reduced part weight.

Table 8. Response table values for part weight

Level	A (mm)	B (%)	C (mm)	D (°)
1	-30.42	-28.41	-30.54	-30.65
2	-31.04	-31.15	-30.87	-31.14
3	-31.29	-33.19	-31.34	-30.96
Delta	0.87	4.78	0.80	0.49
Rank	2	1	3	4

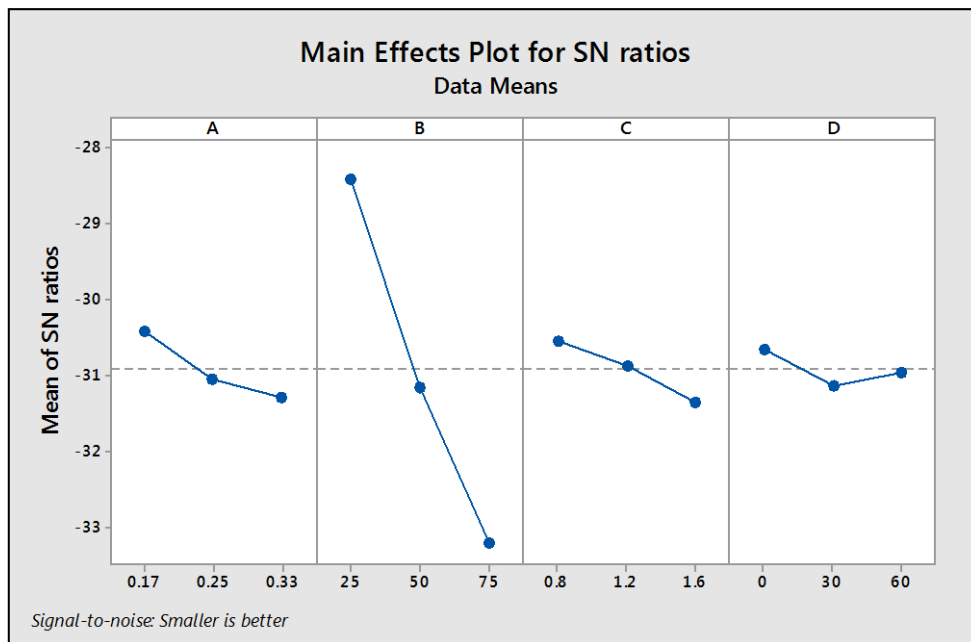


Figure 6. Main effect plot for reduced specimen weight

3.4. Flexural modulus

Flexural modulus is one of the mechanical property of printed part's for the applications where high flexural modulus is in demand. The ratio between flexural strength to strain in the elastic domain is termed as flexural modulus. The main effect plot shows that 0.17 mm layer thickness, 75% infill density, 1.2 mm shell thickness and raster angle of 30° can improve the flexural modulus of the printed part to a greater extent. Ajay kumar et.al [12] highlighted that no factor is found to have significance over flexural strength for carbon fibre reinforced PET-G which includes layer thickness and infill density in his study. But from the current study response table indicates raster angle as highly significant parameter in case of flexural modulus and significance or severity further reduces in the order of layer thickness, infill density and shell thickness. Table 9 shows the response values for flexural modulus and Figure 7 represents its main effect plot.

Table 9. Response table values for flexural modulus

Level	A (mm)	B (%)	C (mm)	D (°)
1	21.32	18.68	20.91	18.05
2	20.63	20.38	19.06	21.73
3	18.31	21.21	20.31	20.49
Delta	3.01	2.54	1.83	3.68
Rank	2	3	4	1

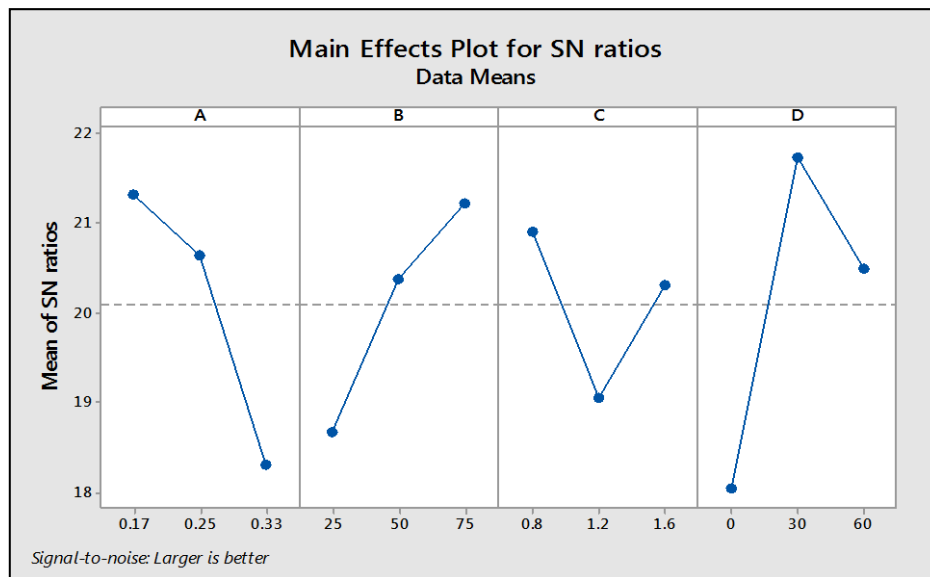


Figure 7. Main effect plot for improved flexural modulus

3.5. Multi response optimization

Multi response optimization is a broad area in research which focusses primarily on simultaneous optimization of input parameters to understand its potential significance over the multiple responses involved in a study. The study gets started by finding the weights of the individual responses based upon the associated category or criteria. The involved responses involved are categorized as beneficial and non beneficial criteria. In the case of manufacturing process, manufacturing time, cost, material waste etc are considered to be non beneficial if they are increasing and factors like properties of the material such as strength, hardness, surface quality characteristics such as surface finish are considered to be beneficial if they are in increasing mode. The weightages of individual criteria or responses could be calculated through standard procedures or may be randomly assigned. Random assigning of criteria weights may lead to inaccuracies in the optimization study. The current study involves two non beneficial criteria, such as printing time and part weight, which has to be reduced. Flexural modulus as the beneficial criterion which has to be increased through optimized parameter settings.

In the current study, weightages of responses have been obtained using Shannon’s entropy and CRITIC method. The weightage of the individual responses has been calculated to convert the normalized values of responses to weighted normalized values for obtaining the ranking of alternatives. Table 10 shows the weightages for the output responses obtained through Shannon’s entropy and CRITIC methods. As for entropy method printing time has got 37% weightage followed by flexural modulus with 36% weightage and part weight with 28%. But as for CRITIC method flexural modulus has got 43% weightage, part weight with 29% and printing time with 28% weightages.

Table 10. Weightages of output responses through entropy and CRITIC methods

S. No	Output Responses	Entropy	CRITIC
1	Printing time	0.37	0.28
2	Part weight	0.28	0.29
3	Flexural Modulus	0.36	0.43



3.6. Grey Relational Analysis (GRA)

Grey relational analysis is a method for determining the optimum conditions of various input factors along with their levels for obtaining desired output characteristics of a product or a process. The values of the measured output parameters are first converted into normalized values based upon the category of output parameters and multiplied by corresponding weights to obtain the weighted normalized values. The values of deviation sequence are further assessed for individual parameters to ascertain the value of grey relational coefficient. The average of grey relational coefficient provides the value of grey relational grade which has to be ranked in descending order for obtaining the ranking of alternatives considered in the study. Tables 11 and 12 show the ranking of alternatives, optimized parameter settings and ranking of input parameters obtained as per GRA – Entropy Method.

Table 11. Ranking of alternatives by GRA – entropy method

Trial No	Normalized values			Weighted normalized values			Deviation sequence			Grey relational coefficient			Grey relational grade	Rank
	PT (mins)	PW (gms)	FM (GPa)	PT (mins)	PW (gms)	FM (GPa)	PT (mins)	PW (gms)	FM (GPa)	PT (mins)	PW (gms)	FM (GPa)		
1	0.7500	1.0000	0.2081	0.2775	0.2800	0.0749	0.0925	0.0000	0.2851	0.6667	1.0000	0.3870	0.6846	1
2	0.3516	0.4868	0.6577	0.1301	0.1363	0.2368	0.2399	0.1437	0.1232	0.4354	0.4935	0.5936	0.5075	6
3	0.0000	0.0175	0.7954	0.0000	0.0049	0.2863	0.3700	0.2751	0.0737	0.3333	0.3373	0.7096	0.4601	8
4	0.8984	0.8421	0.1996	0.3324	0.2358	0.0719	0.0376	0.0442	0.2881	0.8312	0.7600	0.3845	0.6586	3
5	0.6641	0.3772	0.2535	0.2457	0.1056	0.0913	0.1243	0.1744	0.2687	0.5981	0.4453	0.4011	0.4815	7
6	0.5469	0.0175	1.0000	0.2023	0.0049	0.3600	0.1677	0.2751	0.0000	0.5246	0.3373	1.0000	0.6206	4
7	1.0000	0.7149	0.2166	0.3700	0.2002	0.0780	0.0000	0.0798	0.2820	1.0000	0.6369	0.3896	0.6755	2
8	0.9297	0.4211	0.3330	0.3440	0.1179	0.1199	0.0260	0.1621	0.2401	0.8767	0.4634	0.4284	0.5895	5
9	0.7578	0.0000	0.0000	0.2804	0.0000	0.0000	0.0896	0.2800	0.3600	0.6737	0.3333	0.3333	0.4468	9

Table 12. Optimized parameter settings and ranking of input parameters by level totals GRA – entropy

Parameters	1	2	3	Max-Min	Rank
A	1.6522	1.7607	1.7118	0.06	4
B	2.0186	1.5786	1.5275	0.49	1
C	1.8947	1.6128	1.6171	0.28	2
D	1.6129	1.8036	1.7082	0.19	3

Table 13. Ranking of alternatives by GRA – CRITIC method

Trial No	Normalized values			Weighted normalized values			Deviation sequence			Grey relational coefficient			Grey relational grade	Rank
	PT (mins)	PW (gms)	FM (GPa)	PT (mins)	PW (gms)	FM (GPa)	PT (mins)	PW (gms)	FM (GPa)	PT (mins)	PW (gms)	FM (GPa)		
1	0.7500	1.0000	0.2081	0.2100	0.2900	0.0895	0.0700	0.0000	0.3405	0.6667	1.0000	0.3870	0.6846	1
2	0.3516	0.4868	0.6577	0.0984	0.1412	0.2828	0.1816	0.1488	0.1472	0.4354	0.4935	0.5936	0.5075	6
3	0.0000	0.0175	0.7954	0.0000	0.0051	0.3420	0.2800	0.2849	0.0880	0.3333	0.3373	0.7096	0.4601	8
4	0.8984	0.8421	0.1996	0.2516	0.2442	0.0858	0.0284	0.0458	0.3442	0.8312	0.7600	0.3845	0.6586	3
5	0.6641	0.3772	0.2535	0.1859	0.1094	0.1090	0.0941	0.1806	0.3210	0.5981	0.4453	0.4011	0.4815	7
6	0.5469	0.0175	1.0000	0.1531	0.0051	0.4300	0.1269	0.2849	0.0000	0.5246	0.3373	1.0000	0.6206	4



7	1.0000	0.7149	0.2166	0.2800	0.2073	0.0932	0.0000	0.0827	0.3368	1.0000	0.6369	0.3896	0.6755	2
8	0.9297	0.4211	0.3330	0.2603	0.1221	0.1432	0.0197	0.1679	0.2868	0.8767	0.4634	0.4284	0.5895	5
9	0.7578	0.0000	0.0000	0.2122	0.0000	0.0000	0.0678	0.2900	0.4300	0.6737	0.3333	0.3333	0.4468	9

Table 14. Optimized parameter settings and ranking of input parameters by level totals GRA – CRITIC

Parameters	1	2	3	Max-Min	Rank
A	1.6522	1.7607	1.7116	0.11	4
B	2.018	1.5786	1.5275	0.49	1
C	1.894	1.6128	1.6171	0.28	2
D	1.612	1.8036	1.7082	0.19	3

Tables 13 and 14 represent the ranking of alternatives and optimized parameter settings according to GRA - CRITIC method. From the methods combined such as GRA - Entropy and GRA - CRITIC the optimized combination of parameter settings through the ranking of alternatives is found to be A1B1C1D1 (Experiment no : 1- 0.17 mm layer thickness, 25% infill density, 0.8 mm shell thickness and 0° raster angle). The optimized setting recommended from level totals is same from both the methods A2B1C1D2 (0.25 mm layer thickness, 25% infill density, 0.8 mm shell thickness and 30° raster angle) but vary while comparing with the ranking of alternatives. Infill density ranks top with higher significance, followed by shell thickness, raster angle and layer thickness from both the methods considered.

3.7. Technique of order preference similar to ideal solution (TOPSIS)

TOPSIS stands for technique for order of preference by similarity to ideal solution, is a multi-criteria decision analysis method. It compares a set of alternatives based on a pre-specified criterion. The method has been used in diverse domains when an analytical decision needs to be arrived based upon collected data. The general logic of TOPSIS is based on the concept that the chosen alternative should have shortest geometric distance from the best solution and the longest geometric distance from the worst solution.

Table 15. Ranking of alternatives by TOPSIS – Entropy Method

Trial No	Normalized values			Weighted normalized values			Positive Ideal Solution	Negative Ideal Solution	Closeness coefficient	Rank
	PT (mins)	PW (gms)	FM (GPa)	PT (mins)	PW (gms)	FM (GPa)				
1	0.2896	0.2084	0.2620	0.1071	0.0583	0.0943	0.0887	0.1074	0.5476	5
2	0.4158	0.3139	0.3940	0.1539	0.0879	0.1419	0.0892	0.0856	0.4896	6
3	0.5272	0.4104	0.4345	0.1951	0.1149	0.1564	0.1319	0.0841	0.3893	9
4	0.2426	0.2408	0.2595	0.0897	0.0674	0.0934	0.0860	0.1179	0.5782	4
5	0.3168	0.3365	0.2753	0.1172	0.0942	0.0991	0.0952	0.0851	0.4720	7
6	0.3539	0.4104	0.4946	0.1310	0.1149	0.1781	0.0776	0.1237	0.6145	1
7	0.2104	0.2670	0.2645	0.0778	0.0748	0.0952	0.0845	0.1263	0.5993	2
8	0.2327	0.3274	0.2986	0.0861	0.0917	0.1075	0.0785	0.1171	0.5987	3
9	0.2871	0.4140	0.2008	0.1062	0.1159	0.0723	0.1237	0.0888	0.4179	8

Table 15 shows the ranking of alternatives obtained for TOPSIS - entropy method and the parameter setting A2B3C1D2 is found to be the optimized setting for desired output characteristics.

Table 16. Optimized parameter settings and ranking of input parameters by level totals TOPSIS – entropy method

Parameters	1	2	3	Max-Min	Rank
A	1.4265	1.6647	1.616	0.238	4
B	1.7251	1.5603	1.4217	0.303	1
C	1.7607	1.4857	1.4607	0.300	2
D	1.4375	1.7033	1.5663	0.266	3

Table 16 shows the optimized parameter setting as per level totals of input factors for TOPSIS – Entropy method and the parameter setting A2B1C1D2 is found to be the optimized combination of parameters. Infill density ranks top followed by shell thickness, raster angle and layer thickness.

Table 17. Ranking of alternatives by TOPSIS – CRITIC method

Trial No	Normalized values			Weighted normalized values			Positive Ideal Solution	Negative Ideal Solution	Closeness coefficient	Rank
	PT (mins)	PW (gms)	FM (GPa)	PT (mins)	PW (gms)	FM (GPa)				
1	0.2896	0.2084	0.2620	0.0811	0.0604	0.1126	0.1025	0.0931	0.4762	7
2	0.4158	0.3139	0.3940	0.1164	0.0910	0.1694	0.0782	0.0934	0.5442	2
3	0.5272	0.4104	0.4345	0.1476	0.1190	0.1868	0.1094	0.1005	0.4787	6
4	0.2426	0.2408	0.2595	0.0679	0.0698	0.1116	0.1019	0.0975	0.4889	5
5	0.3168	0.3365	0.2753	0.0887	0.0976	0.1184	0.1056	0.0707	0.4010	8
6	0.3539	0.4104	0.4946	0.0991	0.1190	0.2127	0.0711	0.1353	0.6557	1
7	0.2104	0.2670	0.2645	0.0589	0.0774	0.1137	0.1004	0.1022	0.5043	4
8	0.2327	0.3274	0.2986	0.0651	0.0950	0.1284	0.0913	0.0959	0.5124	3
9	0.2871	0.4140	0.2008	0.0804	0.1201	0.0864	0.1413	0.0672	0.3223	9

Table 18. Optimized parameter settings and ranking of input parameters by level totals TOPSIS – CRITIC method

Parameters	1	2	3	Max-Min	Rank
A	1.4991	1.5456	1.3391	0.21	3
B	1.4694	1.4577	1.4567	0.01	4
C	1.6443	1.3555	1.3841	0.29	2
D	1.1995	1.7043	1.4801	0.50	1

Table 17 shows the ranking of alternatives obtained and Table 18 represents the optimized parameter settings through level totals through TOPSIS –CRITIC method. The ranking of alternatives through TOPSIS - Entropy and TOPSIS - CRITIC methods is found to be same with A2B3C1D2 (Experiment No 6 - 0.25 mm layer thickness, 75% infill density, 0.8 mm shell thickness and 30° raster angle) but the level totals recommend the same setting A2B1C1D2 (0.25 mm layer thickness, 25% infill density, 0.8 mm shell thickness and 30° raster angle) in similar to previously combined methods. The ranking of parameters vary from both the methods, TOPSIS - Entropy highlights infill density with top ranking followed by shell thickness, raster angle and layer thickness in accordance with GRA-Entropy and GRA - CRITIC methods. TOPSIS - CRITIC ranks raster angle in the top, shell thickness as second, layer thickness as third and infill density as the least significant one. Table 19 shows the summary of optimized parameter settings obtained.

Table 19. Summary of optimized parameter settings and significant input factors

S. No	Method(s)	Optimized setting(s)(ranking of alternatives)	Optimized Setting(s) (Level Totals)	Highly Significant	Low Significant
1	GRA - Entropy	A1B1C1D1	A2B1C1D2	Infill Density	Layer Thickness
2	GRA - CRITIC	A1B1C1D1	A2B1C1D2	Infill Density	Layer Thickness
3	TOPSIS - Entropy	A2B3C1D2	A2B1C1D2	Infill Density	Layer Thickness
4	TOPSIS -CRITIC	A2B3C1D2	A2B1C1D2	Raster Angle	Infill Density

From the optimized parameter settings obtained through ranking and level total the combinations recommended through ranking of TOPSIS – Entropy & CRITIC methods (A2B3C1D2) and by level totals of all the four different methods considered (A2B1C1D2) have been taken for validation through confirmation trials. Figure 8 shows the specimen prepared for validating the parameter settings through confirmation trials.

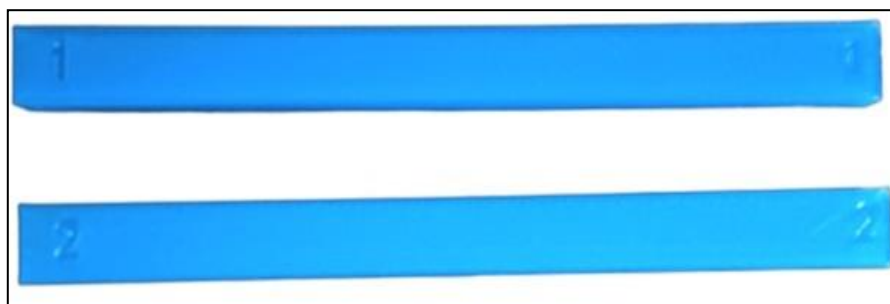


Figure 8. 3D Printed PET-G specimens for confirmation trials

Table 20. Results of optimized parameter settings - confirmation trials

No.	Method(s)	Optimized setting	A (mm)	B (%)	C (mm)	D (°)	PT (mins)	SW (gms)	FM (Gpa)
1	TOPSIS-ENTROPY & CRITIC (Ranking of Alternative)	A2B3C1D2	0.25	75	0.8	30	147	44.5	30.36
2	GRA-ENTROPY & CRITIC TOPSIS-ENTROPY & CRITIC (Level Totals)	A2B1C1D2	0.25	25	0.8	30	90	25	20.44

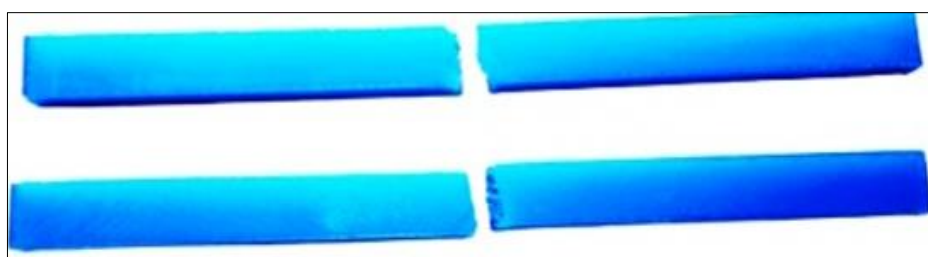


Figure 9. Fractured PET-G specimens after confirmation trials

Table 20 shows the results obtained through optimized parameter settings. Figure 9 shows the fractured flexural specimen after confirmation test. From the results of confirmation trials carried out for validation of the optimized settings obtained the setting A2B3C1D2 has shown maximum flexural modulus of 30.36 GPa, at printing time of 147 min with 44.5 g part weight and the setting A2B1C1D2 has shown minimum printing time of 90 min with part weight of 25 g and flexural modulus of 20.44

GPa. In both settings arrived from different methods, only infill density has got a change from 75 to 25% and all other factors remained constant. Printing time decreases by 38.77%, part weight decreases by 43.8% and flexural modulus gets decreased by 32.67% when the infill density is decreases from 75 to 25%.

4. Conclusions

The study involves the experimental investigation of flexural modulus for PET-G material manufactured through fused deposition modeling and the evaluation of printing time, part weight. The conducted study involves mono and multi response optimization for identifying the significant, non - significant input parameter affecting the responses and optimized parameter setting which can increase or decrease the output response as per industrial requirements. The concluding remarks of the study are detailed below for better understanding.

From the experimental work carried out and its observations, the lowest printing time of 85 minutes for making the part is obtained from A3B1C3D2 (0.33 mm layer thickness, 25% infill density, 1.6 mm shell thickness and 30° raster angle). The specimen weighs less with 23.1 g for A1B1C1D1 (0.17 mm layer thickness, 25% infill density, 0.8 mm shell thickness and 0° raster angle) and the minimum flexural modulus of 6.58 GPa is recorded with A3B3C2D1 (0.33 mm layer thickness, 75% infill density, 1.2 mm shell thickness and 0° raster angle).

The maximum printing time for specimen of 213 min is obtained from A1B3C3D3 (0.17 mm layer thickness, 75% infill density, 1.6 mm shell thickness and 60° raster angle) and the part weighs more with 45.9 g from A3B3C2D1 (0.33 mm layer thickness, 75% infill density, 1.2 mm shell thickness and 0° raster angle). Higher flexural strength of 16.21 GPa is obtained for the specimen printed using the settings A2B3C1D2 (0.25 mm layer thickness, 75% infill density, 0.8 mm shell thickness and 30° raster angle).

Through mono optimization study by adopting signal to noise ratio method, for both printing time and part weight raster angle is less significant but it ranks in top in the case of flexural modulus. The layer thickness is significant for reducing printing time and infill density is significant for part weight reduction.

The weightages for the responses considered in the study varies depending on the method considered for evaluation. In case of weightage, entropy method recommends 37% for printing time, 28% for part weight and 36% for flexural modulus. But CRITIC method declares 28% for printing time, 29% for part weight and 43% for flexural modulus. The weightage of output responses varies from method to method in a considerable manner.

The combined methods such as GRA - Entropy, GRA - CRITIC and TOPSIS - Entropy indicates infill density as the highly significant parameter affecting the responses and layer thickness is found to have very low significance. TOPSIS - CRITIC indicates raster angle as the most significant parameter and infill density as the least significant one.

Irrespective of the adopted combined method, shell thickness ranks at the second position as the significant influencing factor over the combined response study.

The ranking of alternatives obtained through the combined methods such as GRA - Entropy and GRA- CRITIC is found to be similar A1B1C1D1 (0.17 mm layer thickness, 25% infill density, 0.8 mm shell thickness and 0° raster angle). The ranking of alternatives obtained through TOPSIS - Entropy and TOPSIS – CRITIC method is found to have the optimized parameter setting A2B3C1D2 (0.25 mm layer thickness, 75% infill density, 0.8 mm shell thickness and 30° raster angle).

The optimized parameter settings obtained from the level total of input parameters are found to have a very good agreement between all the methods considered (GRA - Entropy, GRA- CRITIC, TOPSIS - Entropy and TOPSIS - CRITIC). A2B1C1D2 (0.25 mm layer thickness, 25% infill density, 0.8 mm shell thickness and 30° raster angle) is the optimized parameter setting recommended.

The carried - out confirmation trials carried have shown the significance of infill density over the output parameters when it changes from 75 to 25% by holding all other parameters at constant level. All



the three output parameters such as printing time, part weight and flexural modulus that decreased by 38.77, 43.8 and 32.67% respectively when the infill density is decreased.

Infill density is the most significant parameter affecting all the responses than other studied input factors.

References

- 1.S. N. MAZURCHEVICI *et al.*, Technological parameters effects on mechanical properties of biodegradable materials using FDM, *Mater. Plast.*, **57**(2), 2020, 215–227 [doi: 10.37358/MP.20.2.5368](https://doi.org/10.37358/MP.20.2.5368).
- 2.C. K. Chua, K. F. Leong, J., An, Introduction to rapid prototyping of biomaterials, *Rapid Prototyping of Biomaterials: Techniques in Additive Manufacturing*, pp. 1–15, 2019, [doi: 10.1016/B978-0-08-102663-2.00001-0](https://doi.org/10.1016/B978-0-08-102663-2.00001-0).
- 3.R. KUMAR, M. KUMAR, J. S. CHOHAN, Material-specific properties and applications of additive manufacturing techniques: a comprehensive review, *Bulletin of Materials Science*, vol. 44, no. 3, 2021, [doi: 10.1007/s12034-021-02364-y](https://doi.org/10.1007/s12034-021-02364-y).
- 4.Z. LIU, Y. WANG, B. WU, C. CUI, Y. GUO, C. YAN, A critical review of fused deposition modeling 3D printing technology in manufacturing polylactic acid parts, *International Journal of Advanced Manufacturing Technology*, vol. 102, no. 9-12, pp. 2877–2889, 2019, [doi: 10.1007/s00170-019-03332-x](https://doi.org/10.1007/s00170-019-03332-x).
- 5.W. AMEEN, S. H. MIAN, H. ALKHALEFAH, Design the support structures for fused deposition modeling 3D printing, *Proceedings of the International Conference on Industrial Engineering and Operations Management*, no. November, pp. 814-825, 2019.
- 6.S. D. NATH, S. NILUFAR, An overview of additive manufacturing of polymers and associated composites, *Polymers*, vol. 12, no. 11, pp. 1–33, 2020, [doi: 10.3390/polym12112719](https://doi.org/10.3390/polym12112719).
- 7.X. GAO, S. QI, X. KUANG, Y. SU, J. LI, D. WANG, Fused filament fabrication of polymer materials: A review of interlayer bond, *Additive Manufacturing*, no. 2, p. 101658, 2020, [doi: 10.1016/j.addma.2020.101658](https://doi.org/10.1016/j.addma.2020.101658).
- 8.R. SRINIVASAN, W. RUBAN, A. DEEPANRAJ, R. BHUVANESH, T. BHUVANESH, Effect on infill density on mechanical properties of PETG part fabricated by fused deposition modelling, *Materials Today: Proceedings*, vol. 27, no. xxxx, pp. 1838-1842, 2020, [doi: 10.1016/j.matpr.2020.03.797](https://doi.org/10.1016/j.matpr.2020.03.797).
- 9.J. M. BARRIOS, P. E. ROMERO, Improvement of surface roughness and hydrophobicity in PETG parts manufactured via fused deposition modeling (FDM): An application in 3D printed self-cleaning parts, *Materials*, vol. 12, no. 15, 2019, [doi: 10.3390/ma12152499](https://doi.org/10.3390/ma12152499).
- 10.F. A. SANTOS *et al.*, Low velocity impact response of 3D printed structures formed by cellular metamaterials and stiffening plates: PLA vs. PETg, *Composite Structures*, vol. 256, no. October 2020, 2021, [doi: 10.1016/j.compstruct.2020.113128](https://doi.org/10.1016/j.compstruct.2020.113128).
- 11.R. SRINIVASAN, P. PRATHAP, A. RAJ, S. A. KANNAN, V. DEEPAK, Influence of fused deposition modeling process parameters on the mechanical properties of PETG parts, *Materials Today: Proceedings*, vol. 27, no. xxxx, pp. 1877-1883, 2020, [doi: 10.1016/j.matpr.2020.03.809](https://doi.org/10.1016/j.matpr.2020.03.809).
- 12.M. A. KUMAR, M. S. KHAN, S. B. MISHRA, Effect of machine parameters on strength and hardness of FDM printed carbon fiber reinforced PETG thermoplastics, *Materials Today: Proceedings*, vol. 27, no. xxxx, pp. 975–983, 2020, [doi: 10.1016/j.matpr.2020.01.291](https://doi.org/10.1016/j.matpr.2020.01.291).
- 13.R. SRINIVASAN, K. NIRMAL KUMAR, A. JENISH IBRAHIM, K. V. ANANDU, R. GURUDHEVAN, Impact of fused deposition process parameter (infill pattern) on the strength of PETG part, *Materials Today: Proceedings*, vol. 27, no. xxxx, pp. 1801-1805, 2020, [doi: 10.1016/j.matpr.2020.03.777](https://doi.org/10.1016/j.matpr.2020.03.777).
- 14.M. M. HANON, R. MARCZIS, L. ZSIDAI, Anisotropy evaluation of different raster directions, spatial orientations, and fill percentage of 3d printed petg tensile test specimens, *Key Engineering Materials*, vol. 821 KEM, pp. 167-173, 2019, [doi: 10.4028/www.scientific.net/KEM.821.167](https://doi.org/10.4028/www.scientific.net/KEM.821.167).
- 15.A. ÖZEN, D. AUHL, C. VÖLLMECKE, J. KIENDL, B. E. ABALI, Optimization of Manufacturing Parameters and Tensile, *Materials*, 2021.



- 16.K. DURGASHYAM, M. INDRA REDDY, A. BALAKRISHNA, K. SATYANARAYANA, Experimental investigation on mechanical properties of PETG material processed by fused deposition modeling method, *Materials Today: Proceedings*, vol. 18, no. xxxx, pp. 2052-2059, 2019, doi: [10.1016/j.matpr.2019.06.082](https://doi.org/10.1016/j.matpr.2019.06.082).
- 17.M. S. SRINIDHI, R. SOUNDARARAJAN, K. S. SATISHKUMAR, S. SURESH, Enhancing the FDM infill pattern outcomes of mechanical behavior for as-built and annealed PETG and CFPETG composites parts , *Materials Today: Proceedings*, vol. 45, no. xxxx, pp. 7208-7212, 2020, doi: [10.1016/j.matpr.2021.02.417](https://doi.org/10.1016/j.matpr.2021.02.417).
- 18.M. H. HSUEH *et al.*, Effect of printing parameters on the thermal and mechanical properties of 3d-printed pla and petg, using fused deposition modeling, *Polymers*, vol. 13, no. 11, 2021, doi: [10.3390/polym13111758](https://doi.org/10.3390/polym13111758).
- 9.J.M. MERCADO-COLMENERO, M. DOLORES LA RUBIA, E. MATA-GARCIA, M. RODRIGUEZ-SANTIAGO, C. MARTIN-DOÑATE, Experimental and numerical analysis for the mechanical characterization of petg polymers manufactured with fdm technology under pure uniaxial compression stress states for architectural applications, *Polymers*, vol. 12, no. 10, pp. 1-25, 2020, doi: [10.3390/polym12102202](https://doi.org/10.3390/polym12102202).
- 20.A. ÖZEN, B. E. ABALI, C. VÖLLMECKE, J. GERSTEL, D. AUHL, Exploring the Role of Manufacturing Parameters on Microstructure and Mechanical Properties in Fused Deposition Modeling (FDM) Using PETG , *Applied Composite Materials*, vol. 28, no. 6, pp. 1799-1828, 2021, doi: [10.1007/s10443-021-09940-9](https://doi.org/10.1007/s10443-021-09940-9).
- 21.D. YADAV, D. CHHABRA, R. K. GUPTA, A. PHOGAT, A. AHLAWAT, Modeling and analysis of significant process parameters of FDM 3D printer using ANFIS, *Materials Today: Proceedings*, vol. 21, no. xxxx, pp. 1592-1604, 2020, doi: [10.1016/j.matpr.2019.11.227](https://doi.org/10.1016/j.matpr.2019.11.227).
- 22.N. MOHAMMED RAFFIC, K. GANESH BABU, S. SELVAKUMAR, S. RADHAKRISHNAN, Experimental Investigation on the Effect of Fused Deposition Modelling Parameters for HIPS Material by Experimental Design and MRO Techniques, *IOP Conference Series: Materials Science and Engineering*, vol. 988, no. 1, 2020, doi: [10.1088/1757-899X/988/1/012051](https://doi.org/10.1088/1757-899X/988/1/012051).
- 23.N. M. RAFFIC, K. G. BABU, P. MADHAN, Application of taguchi's experimental design and range analysis in optimization of FDM printing parameters for PET-G, PLA and HIPS, *International Journal of Scientific and Technology Research*, vol. 8, no. 9, pp. 891-902, 2019.
- 24.N. M. RAFFIC, K. G. BABU, A. KUMARAN, G. R. KIRAN, Parametric Optimization Study of ABS Material Using FDM Technique for Fatigue Life Prediction, vol. 6, no. 11, pp. 4-11, 2018.
- 25.N. M. RAFFIC, K. G. BABU, A. C. ASHIQ, Pilot Testing of FDM Samples by Taguchi's L 4 Orthogonal Array and Multi Response Optimization using GRA and DEAR Approaches, no. May, pp. 1438-1450, 2020.
- 26.H. HADIDI, *et al.*, Low velocity impact of ABS after shot peening predefined layers during additive manufacturing, *Procedia Manufacturing*, vol. 34, pp. 594-602, 2019, doi: [10.1016/j.promfg.2019.06.169](https://doi.org/10.1016/j.promfg.2019.06.169).

Manuscript received: 29.01.2022